Hydrol. Earth Syst. Sci. Discuss., 11, 9435–9473, 2014
www.hydrol-earth-syst-sci-discuss.net/11/9435/2014/
doi:10.5194/hessd-11-9435-2014

Hydrology and Earth System Sciences
Discussions
Open Access

The Budyko and complementary relationships in an idealized model of large-scale land–atmosphere coupling

B. R. Lintner[1], P. Gentine[2], K. L. Findell[3], and G. D. Salvucci[4]

[1]Department of Environmental Sciences, Rutgers, The State University of New Jersey, New Brunswick, NJ, USA
[2]Department of Earth and Environmental Engineering and Earth Institute, Columbia University, New York, NY, USA
[3]Geophysical Fluid Dynamics Laboratory, Princeton, NJ, USA
[4]Department of Earth and Environment, Boston University, Boston, MA, USA

Received: 15 May 2014 – Accepted: 16 June 2014 – Published: 7 August 2014

Correspondence to: B. R. Lintner (lintner@envsci.rutgers.edu)

Published by Copernicus Publications on behalf of the European Geosciences Union.

Abstract

Expressions corresponding to two well-known relationships in hydrology and hydrometeorology, the Budyko and complementary relationships, are derived within an idealized prototype representing the physics of large-scale land–atmosphere coupling. These relationships are shown to hold on long (climatologic) time scales because of the tight coupling that exists between precipitation, atmospheric radiation, moisture convergence and advection. The slope of the complementary relationship is shown to be dependent the Clausius–Clapeyron relationship between saturation specific humidity and temperature, with important implications for the continental hydrologic cycle in a warming climate, e.g., one consequence of this dependence is that the complementary relationship may be expected to become more asymmetric with warming, as higher values of the slope imply a larger change in potential evaporation for a given change in evapotranspiration. In addition, the transparent physics of the prototype permits diagnosis of the sensitivity of the Budyko and complementary relationships to various atmospheric and land surface processes. Here, the impacts of anthropogenic influences, including large-scale irrigation and global warming, are assessed.

1 Introduction

Observations of the annual terrestrial surface water balance demonstrate a tight and relatively simple functional dependence of evapotranspiration on the atmospheric water supply (precipitation) and demand (potential evaporation) at the surface (Budyko, 1961; Porporato et al., 2004; Roderick and Farquahr, 2011; Williams et al., 2012; Zanardo et al., 2012). Such observations have stimulated development of simplified analytical formulations of the annual water balance (Budyko, 1961; Lettau, 1961; Eagleson, 1978a, b, c; Fu, 1981; Milly, 1994; Porporato et al., 2004; Harman et al., 2011; Sivapalan et al., 2011). Budyko (1961, 1974) developed arguably the most well-known approach for characterizing catchment-scale hydrologic balances on long (decadal and

HESSD
11, 9435–9473, 2014

greater) timescales. By hypothesizing limitations on land surface evapotranspiration imposed by the availability of water and energy, Budyko introduced a relationship of the form:

$$\frac{E}{P} = B\left(\frac{E_p}{P}\right) \tag{1}$$

where E, P, and E_p are evapotranspiration, potential evapotranspiration, and precipitation, respectively. The ratio E_p/P is commonly known as the dryness or aridity index (ϕ), and hereafter we denote the ratio E/P as $B(\phi)$, i.e., the Budyko curve. Empirical forms of $B(\phi)$ have been obtained by fitting to observed E, P, and E_p with E typically estimated as the residual of precipitation and basin-scale streamflow (Budyko, 1961, 1974). $B(\phi)$ appears to be rather stable across different regions and hydroclimatic environments (Potter et al., 2005; Yang et al., 2007; Gentine et al., 2012).

The last two decades have seen renewed interest in the Budyko curve (Milly, 1994; Koster and Suarez, 1999; Milly and Dunne, 2002; Porporato et al., 2004; Potter et al., 2005; Donohue et al., 2007; Yang et al., 2008; Gerrits et al., 2009; Gentine et al., 2012; Istanbulluoglu et al., 2012; Williams et al., 2012). Many studies have employed simplified models of the surface and groundwater moisture response to precipitation forced by potential evapotranspiration to investigate the robustness of the Budyko curve in different catchments. Milly (1994) and Porporato et al. (2004), in particular, investigated the response of the annual water balance to changes in the characteristics of potential evaporation and precipitation intensity and frequency yielding new insights on the sensitivity of the annual water balance to changes in surface energy and water forcing, all other factors, e.g., vegetation characteristics, soil, topography, remaining constant. However, apart from a few studies investigating the catchment co-evolution and adaptation of vegetation to the water and energy forcing (Troch et al., 2009; Sivapalan et al., 2011; Gentine et al., 2012), a direct explanation of the stability and widespread applicability of the Budyko relationship across a range of conditions remains elusive.

HESSD
11, 9435–9473, 2014

In the Budyko framework, as in most hydrologic models, potential evaporation is prescribed as a forcing, which is thought to be independent from the surface. Nonetheless, E and E_p and have been shown to be inversely related to one another (Bouchet, 1963; Morton, 1983; Brutsaert and Stricker, 1979; Hobbins et al., 2001) on daily to annual time scales. In fact, the coupling between E and E_p provides the basis for a foundational relationship in hydrometeorology: the complementary relationship, first introduced by Bouchet (1963) and Morton (1983). Mathematically, the complementary relationship (CR) can be expressed as:

$$E_p + bE = (1 + b)E_{wet}. \tag{2}$$

In Eq. (2), E_p is potential evaporation and E_{wet} is the energy-limited, wet surface equilibrium evapotranspiration. Bouchet (1963) assumed a value of 1 for the scale factor b while Pettijohn and Salvucci (2009) report values in the range 3–6 based on numerical simulations of an evaporation pan in a drying environment. Since E_p cannot directly be measured, pan evaporation has often been used in lieu of potential evaporation using a pan correction factor (Bosman, 1987; Roderick and Farquahr, 2004; van Heerwaarden et al., 2010). Kahler and Brutsaert (2006) assumed that use of pan measurements in Eq. (2) may account for $b > 1$ because a pan transmits heat, resulting in warmer water inside the pan relative to a larger free water body (e.g., lake) under similar ambient conditions.

Although several studies (Zhang et al., 2004; Ramirez et al., 2005; Szilagyi and Jozsa, 2009) have discussed possible links between the complementary relationship and the Budyko curve, to date a theoretical framework encompassing either or both of these relationships is still absent. Milly (1994) notes the lack of physical understanding for why the Budyko curve deviates from its water- and energy-limited asymptotes, while Ramirez et al. (2005) suggest that, apart from heuristic arguments or under restrictive conditions, no general proof of the complementary relationship is available. Moreover, questions remain about the applicability and validity of the Budyko and complementary relationships across different spatial and temporal scales. Here we note that observational data confirm the complementary relationship holds on daily to annual time scales (Bouchet, 1963; Kahler and Brutsaert, 2006) and across local to regional spatial scales (Granger, 1989; Szilagyi, 2001; Crago and Crowley, 2005; Pettijohn and Salvucci, 2009, hereafter PS09; van Heerwaarden et al., 2010), which is usually understood in terms of the diurnal-scale interactions of the boundary layer with the surface, although questions have been raised about some of the assumptions inherent in these approaches. Indeed, as PS09 note, some explanations for the complementary relationship have relied on contradictory assumptions. For example, the derivation of Szilagyi (2001) assumes that as E decreases, the surface temperature of the evaporation pan remains while the overlying near surface specific humidity decreases, increasing the vapor deficit over the pan rate and thereby the rate of pan evaporation. By contrast, in Granger (1989) surface temperature is assumed to increase while specific humidity remains constant, thus also increasing the humidity gradient and pan evaporation. Lhomme and Guilioni (2006) question the applicability and physical validity of these assumptions.

In the present study, we make use of a semi-analytic, idealized prototype of large-scale land–atmosphere coupling developed in prior work (Lintner et al., 2013) to derive the Budyko and complementary relationships. Our approach differs from prior analyses in that (i) it is implicitly large-scale and relevant on climatic timescales, and (ii) convergence, advection, precipitation and atmospheric radiation are treated implicitly rather than as exogenous forcing. The latter renders the atmospheric and surface moisture interactive and tightly coupled vertically but also horizontally – through the effect of adjusting advection and convergence. Several studies have pointed out that such tight coupling between radiation, larger-scale circulation and local surface energy budget is key to understanding locally-observed land–atmosphere interactions (Betts et al., 1996, 2003; Betts and Viterbo, 2005; Betts, 2007a, 2014). The analytic simplicity of the idealized prototype facilitates straightforward diagnosis of factors influencing the large-scale coupling, as highlighted in Lintner et al. (2013).

HESSD
11, 9435–9473, 2014

A key motivation for this study is consideration of how the continental hydrologic cycle, and how the behavior reflected in the Budyko curve and complementary relationship, may respond to anthropogenic influences. Indeed, the projected response of terrestrial hydrologic cycle to various climate change mechanisms in models remains subject to large uncertainties (Sherwood and Fu, 2014). Emergent behaviors such as the Budyko and complementary relationships may provide useful constraints on such uncertainties. For example, Brutsaert and Parlange (1998) have suggested that the complementary relationship may explain the apparent paradox between observed downward trends in pan evapotranspiration over the late 20th century and anticipated increases in evaporation resulting from a more intense hydrologic cycle in a warming atmosphere.

The paper is organized as follows. After providing a brief review of the prototype assumptions and governing equations (Sect. 2), we analyze the generalized Budyko and complementary relationships (Sect. 3) and consider the physical parameters and processes impacting these relationships (Sect. 4). In Sect. 5, we examine how anthropogenic influences such as global warming and large-scale irrigation affect these relationships.

2 Overview of the idealized land–atmosphere coupling prototype

In prior work (Lintner et al., 2013), we developed a semi-analytic prototype for land–atmosphere coupling. We consider steady-state conditions, corresponding to the climatological state of the hydrologic cycle. While the complementary relationship has been shown to hold on multiple time scales, from daily to annual, its justification on long time scales remains elusive. Similarly the Budyko curve was derived – and is valid only – as a climatology considering a multi-annual mean (Budyko, 1974; Gentine et al., 2012).

HESSD
11, 9435–9473, 2014

The atmospheric component of this prototype is based on vertically-integrated tropospheric temperature and moisture equations from the Quasi-equilibrium Tropical Circulation Model (QTCM; Neelin and Zeng, 2000; Zeng et al., 2000), an intermediate level complexity model for the tropical atmosphere:

$$-\mathrm{Ms}\nabla_{\mathrm{H}}\cdot\boldsymbol{v} + P + R_{\mathrm{net}} + H = 0 \tag{3}$$

$$\mathrm{Mq}\nabla_{\mathrm{H}}\cdot\boldsymbol{v} - P + E - \boldsymbol{v}_{\mathrm{q}}\cdot\nabla_{\mathrm{H}}q = 0 \tag{4}$$

where ∇_{H} is the horizontal gradient operator; R_{net} is the net column (top of the atmosphere minus surface) radiative heating; Ms and Mq are the dry static stability and moisture stratification and $\nabla_{\mathrm{H}}\cdot\boldsymbol{v}$ is signed positive for low-level convergence; and $\boldsymbol{v}_{\mathrm{q}}$ is the vertically-averaged horizontal wind vector weighted by the moisture vertical structure assumed in QTCM1. (Note that baseline values for parameters such as Ms and Mq are given in Lintner et al., 2013 and references therein. Table 1 summarizes parameter values most relevant to the present study.) The term P in Eqs. (3) and (4) represents the net convective (condensational) heating and drying, respectively; the negative sign in Eq. (4) indicates that precipitation is a net sink of vertically-averaged tropospheric moisture. For the temperature Eq. (3), we have neglected horizontal temperature gradients following the weak temperature gradient assumption (Sobel and Bretherton, 2000; Sobel et al., 2001). Note that all terms appearing in Eqs. (3) and (4) are implicitly scaled to units of mm day^{-1} by absorbing constants such as (specific) heat capacity, latent heat of fusion, and column mass per unit area $\Delta p/g$, where Δp is the tropospheric pressure depth.

A steady balanced surface energy flux constraint, in which the annual-mean ground surface heat flux is neglected, reads:

$$R_{\mathrm{surf}} - E - H = 0 \tag{5}$$

where the net surface radiative heating, R_{surf}, is signed positive downward.

In Lintner et al. (2013), we consider tropospheric temperature (T) as prescribed and solve the system of Eqs. (3)–(5) for q, $\nabla_{\mathrm{H}}\cdot\boldsymbol{v}$, and surface temperature T_{s} for prescribed

HESSD
11, 9435–9473, 2014

large-scale advection. A closed-form, self-consistent solution can be obtained by invoking the steady-state soil moisture budget:

$$P - E - Q_{\text{runoff}} = 0 \tag{6}$$

where Q_{runoff} is the net runoff. For analytic simplicity, we assume a simple bucket model, with an evaporative efficiency, $E/E_{\text{p}} = \beta$, for which we assume a simple linear relationship $\beta = w$ (Porporato et al., 2001, 2004), where w is the dimensionless soil moisture (actual soil moisture normalized by holding capacity). Q_{runoff} is represented as the precipitation rate times a power law of soil moisture, $Q_{\text{runoff}} = Pw^{\eta}$ (Kirchner, 2009). Unless otherwise stated, the exponent $\eta = 4$. The suitability of invoking a single moisture storage variable to represent both basin scale evaporative efficiency and runoff has recently been demonstrated at nine watersheds containing Ameriflux eddy covariance measurements of evaporation and gauged streamflow (Tuttle and Salvucci, 2012).

For analytic simplicity, we consider linearized radiative and surface turbulent fluxes of the form:

$$\begin{aligned}
H &= H_0 + \varepsilon_{\text{H}}(T_{\text{s}} - a_{1\text{s}}T) \\
E &= \beta\left[E_{p_0} + \varepsilon_{\text{H}}(\gamma T s - b_{1\text{s}}q)\right] \\
R_x &= R_{x0} + \varepsilon^{\text{Rx}}_{T_{\text{s}}}T_{\text{s}} + \varepsilon^{\text{Rx}}_{\text{T}}T + \varepsilon^{\text{Rx}}_{\text{q}}q + c_xP.
\end{aligned} \tag{7}$$

Quantities with subscript "0" denote the values about which the fluxes are linearized, with coefficients ε representing the linear sensitivity of fluxes to T, q, and T_{s}. Again we note that T and q denote tropospheric vertical averages of temperature and humidity, with scale factors $a_{1\text{s}}$ and $b_{1\text{s}}$ relating these averages to near surface values appropriate for computation of surface bulk turbulent fluxes. The coefficient γ is the slope of the saturation specific humidity with respect to temperature, as defined via the Clausius–Clapeyron equation. Note that in our usage, specific humidity is implicitly scaled to units of temperature (K) via absorption of the psychrometric constant; thus γ is dimensionless. The radiative fluxes are calculated at the top-of-the-atmosphere and the surface

HESSD
11, 9435–9473, 2014

(x = toa and x = surf), and the coefficients c_x are cloud-radiative forcing sensitivities, with cloud-radiative fluxes assumed to be linearly proportional to the precipitation rate. Precipitation (convective heating in Eq. 3 or convective drying in Eq. 4) is formulated in terms of a Betts and Miller (1986)-type relaxation scheme:

$$P = \max[\varepsilon_c(q - q_c(T)), 0]. \tag{8}$$

Here, $q_c(T)$ is a temperature-dependent moisture threshold and ε_c is the convective adjustment rate coefficient (inversely related to the timescale for convective adjustment τ_c).

3 Overview of the baseline relationships

3.1 Complementary relationship

Figure 1a illustrates the functional relationships between soil moisture and E, E_p, and P of the prototype. The general response of E and E_p with increasing soil moisture, namely E_p decreasing and E (generally) increasing, is consistent with the complementary relationship (Eq. 2). E_p relates to w through the deficit between ambient and saturation specific humidity at the surface (Lintner et al., 2013): the deficit decreases with increasing soil moisture since tropospheric humidity q increases while surface temperature T_s decreases. Figure 2 depicts the results of the prototype against E and E_p observations from Little Washita River Basin near Chickasha, Oklahoma (see Kahler and Brutsaert, 2006 for a full description of the dataset). Here E_p was obtained directly from pan evaporation measurements with a correction factor and E was measured using the Bowen ratio (EBBR) technique. E and E_p are presented in dimensionless units by dividing by the Priestly and Taylor (1972) evaporation, i.e., $E_{wet} = \alpha \frac{\gamma}{1+\gamma} R_{surf}$, where α is a correction factor with an estimated value of ~ 1.26. The prototype complementary relationship shows very good correspondence with both datasets. Of course, we should point out that the prototype was not explicitly configured to represent these locations: as such, the correspondence may be coincidental.

A slight decrease in E is observed for $W \gtrsim 0.7$. To our knowledge such a decrease has not been previously investigated, even though it appears in in situ measurements (Kahler and Brutsaert, 2006; PS09). The decrease in both E and E_p arises from the monotonic decrease in E_p ($\frac{\partial E_\mathrm{p}}{\partial w} < 0$) at large soil moisture pointed out by Lintner et al. (2013). Indeed, in the prototype, increasing soil moisture is a consequence of increasing precipitation, with the latter progressively balanced by higher moisture convergence (c.f., Fig. 3 of Lintner et al., 2013). Increasing moisture convergence is associated with increasing (low-level) humidity, which reduces the surface vapor pressure deficit, which ultimately reduces the potential evaporation E_p. Overall the moisture balance at large soil moisture values implies a greater role for nonlocal processes. On the other hand, at very low soil moisture values, mean precipitation is mostly balanced by E, resulting in a tight link among E, E_p, and w. This explains the success of local coupled land-boundary layer models (Bouchet, 1963; van Heerwarden et al., 2010) in representing the drier regime of the complementary relationship. We also note that at low soil moisture values, precipitation essentially mimics the E response and thus a complementary relationship also exists between precipitation and potential evaporation.

In prior studies of the complementary relationship, a quantity E_wet is introduced to denote the point of convergence of E and E_p under unlimited soil moisture (saturated surface) conditions i.e. at high soil moisture values (see Eq. 2). Conventionally, E_wet is assumed to represent equilibrium E from a saturated surface when advection is minimal and is usually computed empirically following Priestly and Taylor (1972). While the prototype E_p does indeed converge toward E as soil moisture increases, there is in fact no unique value of E_wet because of the decline E at larger soil moisture.

As PS09 further note, plotting potential evapotranspiration and evapotranspiration against soil moisture (or a similar variable) may mask the linear nature of the complementary relationship. Thus, Fig. 1b depicts E_p directly as a function of E. In this case, the approximate linearity implied by Eq. (1) is found to hold over a large range of E and E_p values. A linear regressive best fit to the E_p vs. E curve for $E < 6\,\mathrm{mm\,day^{-1}}$ yields a slope, i.e., the parameter b in Eq. (1) of magnitude ~ 3.8. This value of b is very consistent with the estimates of Kahler and Brutsaert (2006), Szilagyi (2007), and PS09, and unlike the original treatment of Bouchet (with $b = 1$), implies a strongly asymmetric complementary relationship. The implied value of b is close to γ, the dimensionless slope of the saturation specific humidity curve, which is 3.5 in the baseline configuration; as we show in the parameter sensitivity analyses in the following subsection, b varies predominantly with γ, which is consistent with the theoretical arguments presented in Granger (1989).

We can, in fact, derive an analytic expression for the prototype's complementary relationship. We begin by subtracting γH from E_p and invoke the zero surface flux constraint to yield:

$$E_p - \gamma H = E_p + \gamma E - \gamma R_s. \tag{9}$$

Then, using the bulk formulae expressions for E_p and H, the left-hand side of Eq. (9) can be expanded as

$$E_p - \gamma H = \varepsilon_H (a_{1s} \gamma T - b_{1s} q). \tag{10}$$

Since precipitation rate $P = \varepsilon_c (q - q_c(T))$, q can be eliminated in favor of P, which upon rearranging the terms gives:

$$E_p + \gamma E = \gamma R_s - \frac{b_{1s} \varepsilon_H}{\varepsilon_c} P + f(T). \tag{11}$$

In Eq. (11), $f(T)$ is a function of the prescribed temperature profile, defined in terms of the explicitly temperature-dependent quantities and mean values appearing in the linear expansions in Eq. (7), and is thus constant over the transect between dry and humid conditions.

HESSD
11, 9435–9473, 2014

Comparing Eq. (11) to Eq. (2), we find:

$$b = \gamma \tag{12}$$

and

$$E_{\mathrm{wet}} = (1+\gamma)^{-1}\left[\gamma R_{\mathrm{s}} + f(T) - \frac{b_{1\mathrm{s}}\varepsilon_{\mathrm{H}}}{\varepsilon_{\mathrm{c}}}P\right]. \tag{13}$$

As noted above in prior work E_{wet} was defined using the relationship of Priestley and Taylor (1972). The first term of Eq. (13) including the net radiation is analogous to Priestley–Taylor but with a coefficient of 1 in lieu of α. It is worth noting of Kahler and Brutsaert's in situ observations imply a Priestley–Taylor coefficient for E_{wet} in the range of 0.89 to 1.13, which is in line with the value of 1 for the coefficient of E_{wet} suggested by Eq. (13). The second term in E_{wet} represents the temperature dependence of the wet evaporation, which is not explicitly described by the Priestley–Taylor relationship (except to the extent that it appears in net surface radiative heating), though this dependence may implicitly incorporated through variation of α. The last term in the expression for E_{wet} describes a negative feedback of precipitation on E_{wet}, since increasing precipitation is associated with higher tropospheric moisture and thus decreasing vapor pressure deficit at the surface, leading to a lowering of E_{wet}.

It is obvious that E_{wet} as defined by Eq. (13) is not constant across the prototype transect, as it depends on surface radiative heating and precipitation. (In a more general model, variations in tropospheric temperature across the transect would also impact the value of E_{wet}.) Again, we point out that the Priestley–Taylor relationship only shows a dependence on radiation (and the Clausius–Clapeyron slope). In addition to the negative feedback of precipitation on E_{wet} through the vapor deficit, R_{surf} itself also decreases as P increases, owing to the negative cloud-radiative forcing associated with deep convective clouds (see Lintner et al., 2013). Related to the non-constancy of E_{wet}, we also note that value of b differs slightly from the value inferred from fitting over the linear portion of the E_{p} vs. E curve in Fig. 1b.

HESSD
11, 9435–9473, 2014

3.2 Budyko curve

Within the prototype the steady-state soil moisture Eq. (6) can be recast as:

$$B(\phi) = [1 - Q_{\mathrm{runoff}}/P]. \tag{14}$$

For the simple case of a bucket model with $\eta = 2$ and noting that soil moisture can be expressed as $W = \beta(W) = \frac{E}{E_\mathrm{p}} = \frac{B(\phi)}{\phi}$, Eq. (14) reduces to a quadratic equation in $B(\phi)$, with an analytic solution in terms of ϕ expressed as:

$$B(\phi) = \frac{\phi^2}{2}\left(\sqrt{1 + \frac{4}{\phi^2}} - 1\right). \tag{15}$$

Figure 3 illustrates the Budyko curves for the baseline prototype with $\alpha = 4$ and the analytic solution for $\eta = 2$, with Budyko's well-known empirical formulation $B(\phi) = \sqrt{\phi \tanh(\phi^{-1})(1 - e^{-\phi})}$ for comparison. Also depicted are the energy- and water-limited asymptotes. For the baseline configuration, $B(\phi)$ at intermediate values of aridity index lies above the empirical Budyko fit, while the $\eta = 2$ curve lies below. Variation in the shape of $B(\phi)$ with increasing η is consistent with decreasing runoff for a given value of precipitation, which in turn necessitates shifting the surface water balance to favor evapotranspiration. We point out that Eq. (15) possesses limiting behavior consistent with empirically-derived estimates in prior studies (Budyko, 1961; Fu, 1981): $B(\phi) \to 0$ as $\phi \to 0$ with a linear asymptote $B(\phi) \sim \phi$, and $B(\phi) \to 1$ as $\phi \to \infty$ with an asymptote $B(\phi) \sim 1 - \phi^{-1}$.

4 Parameter and process sensitivity

4.1 Parameter sensitivity

We now explore how the complementary relationship depends on parameter values assumed in the prototype. In particular, we focus on how the implied slope of E_p vs.

HESSD
11, 9435–9473, 2014

B. R. Lintner et al.

E depends on a subset of four prototype parameters: the dimensionless slope of the saturation specific humidity curve, γ; the surface drag coefficient, which is embedded in the turbulent flux scaling coefficient εH; the surface cloud longwave forcing, c_{surf}; and the convective adjustment timescale, τ_c. Our consideration of γ as a parameter is motivated by the fact that it controls the Bowen ratio or, similarly, the evaporative fraction (Gentine et al., 2011), and thus the sensitivity of a change in q to a change in T_s. We note that with global warming the saturation specific humidity is expected to increase and thereby modify precipitation and the hydrologic cycle (Held and Soden, 2006). The surface drag coefficient depends on surface roughness and thus may be expected to contribute to heterogeneity in b. c_{surf} and τ_c are associated with two of the more uncertain aspects of atmospheric models, namely the effect of clouds on radiation and the parameterization of deep convection. Although the representation of clouds and convective processes are highly simplified in the prototype, we can view the parameter sensitivity to c_{surf} and τ_c as a guide for anticipating how uncertainty in analogues to these parameters in more complex climate models might affect the complementary relationship.

Figure 4 illustrates the percentage variation of the complementary relationship slope relative to its baseline value as functions of percentage variations in the 4 sensitivity parameters. Each parameter is varied uniformly over a range of ±50 % of its baseline value. It is immediately clear that the slope effectively varies in a 1 : 1 manner with γ. On the other hand, for the other three parameters, the percent variation in the complementary slope is typically an order of magnitude smaller. It is worth noting here the apparent nonlinearity associated with changing the surface drag coefficient, with decreased surface drag associated with proportionally larger reductions in the slope of the complementary relationship compared to increased drag of the same magnitude.

Since γ is just the slope of the Clausius–Clapeyron relationship, it has a quasi-exponential dependence on temperature and thus varies sharply across the range of observed terrestrial temperatures. One consequence of this dependence is that the complementary relationship may be expected to become more asymmetric with

HESSD
11, 9435–9473, 2014

warming, as higher values of the slope imply a larger change in E_p for a given change in E. In turn, this may have implications for the strength of the coupling between the land surface and atmosphere in a warming climate. For example, recent work by Dirmeyer et al. (2012, 2014) points to increases in metrics of land–atmosphere coupling strength in a warming climate. In Sect. 4, we further explore the response of the prototype to a global warming scenario.

We now consider the parameter sensitivity of the Budyko curve for the baseline case. In contrast to the complementary relationship, the Budyko curve is extremely robust, with no apparent change in the shape for these parameter variations. Thus, while E, E_p and P vary in response to changing prototype parameters, their ratios are constrained to move along a fixed Budyko curve, as demonstrated in Sect. 5a. In fact, the analytic solution Eq. (15) and Budyko's empirical formula are both immediately seen to reflect this behavior. Yang et al. (2009) suggest such shape invariance is characteristic of the Budyko curve response to what they term climate condition, as they note climate forcing at a particular location simply moves the system along the existing Budyko curve. By contrast, Yang et al. (2009) show how different locations fall onto distinct Budyko curves as a result of land surface or landscape properties, e.g., vegetation and soil.

4.2 Process intervention experiments

Apart from considering the sensitivity of the CR relationship (or Budyko curves) to parameter values, we can also assess how the prototype solutions respond to altering a particular process or term in the governing equations. For the first such intervention-type experiment, we alter the evapotranspiration (E-intervention) by either prescribing (i) the evaporative efficiency or (ii) potential evapotranspiration to constant values. Experiment (i) is analogous to the methodology adopted in the Global Land Atmosphere Coupling Experiment (GLACE)-type studies for comparing simulations with and without interactive soil moisture (Koster et al., 2004, 2006; Seneviratne et al., 2006). Experiment (ii) is similar to the approach Lintner et al. (2013) used to sever the feedback of near surface climate onto potential evapotranspiration, which here is principally

HESSD
11, 9435–9473, 2014

mediated through suppression of the E_p-dependence on “atmospheric drying power”, since the radiative variation across the prototype transect in the baseline configuration is weak (see discussion below).

Rather than present the complementary relationship directly for the E-intervention experiments (since this necessarily breaks down in either case), we instead show the surface temperature and specific humidity profiles as functions of soil moisture (Fig. 5a and b, respectively). Prescribing evaporative efficiency β (prescribed soil moisture experiment) greatly reduces the variation in surface temperature T_s with soil moisture w (gray curve): while the difference in the baseline T_s (black curve) between the driest and wettest conditions is roughly 5 K, it is under 0.5 K for β prescribed. Similarly, the range of variation in specific humidity (here scaled to a surface value) across soil moisture states is attenuated relative to the baseline, although it is not as pronounced. Qualitatively opposite behavior is evident in T_s and q for prescribed E_p, as the variations of both quantities across the soil moisture states are increased relative to the baseline. Note that at low soil moisture, the behavior of the baseline case more closely resembles the fixed E_p case, while at high soil moisture, it is more like fixed β.

We can further assess how the complementary relationship changes with intervention in either surface sensible heat or radiative flux (Fig. 6). These intervention experiments are implemented by suppressing the relevant dependences of the fluxes on humidity and surface temperature. Under suppression of surface radiative flux (Fig. 6a), there is little net change in the complementary relationship relative to the baseline over most of the soil moisture range; however, at high soil moisture, both E_p and E are slightly increased. In this case, the increase in E_p arises through slightly elevated radiative heating of the surface, since the negative effect of cloud shortwave forcing, i.e., more convective clouds leading to less surface shortwave heating, is absent. This in turn feeds back onto precipitation, which is slightly enhanced. We further mention a competing effect, namely increased surface longwave forcing (and hence warming) with increased water vapor and convective cloudiness. For the parameter values chosen, this effect loses out to the shortwave forcing. On the other hand, uncertainty in

HESSD
11, 9435–9473, 2014

these parameter values, particularly the cloud forcing, could alter the balance of these two effects.

Under suppression of sensible heat flux (Fig. 6b), the complementary relationship is dramatically altered, as E_p drops off more rapidly with increasing soil moisture and E rises faster at low soil moisture and then flattens off (the details of how these curves change depend on the value of sensible heat flux prescribed). Plotting E_p vs. E (not shown) reveals a best fit linear regressive slope of ~ 28, consistent with the very asymmetric nature of the complementary relationship when sensible heat flux variation across the transect is suppressed.

5 Impacts of global warming and large-scale irrigation

5.1 Global warming

How the hydrologic cycle responds to global warming is clearly of great significance to projecting climate change impacts (Allen and Ingram, 2002; Milly et al., 2005). At present, our understanding of the hydrologic cycle response to warming is guided by some theoretical constraints, e.g., the Clausius–Clapeyron relationship promotes enhanced tropospheric moistening, although model projections show considerable spread in the regional signatures of hydrologic cycle change (Held and Soden, 2006; Neelin et al., 2013). Assessing global warming impacts on the terrestrial hydrologic cycle is complicated by changes in land use such as deforestation and agricultural conversion and coupling to vegetation (Lee et al., 2011).

Over the latter half of the 20th century, several studies have reported widespread decreases in pan evaporation (Lawrimore and Peterson, 2000; Hobbins et al., 2004; Roderick and Farquhar, 2004; Shen et al., 2009), which can be related to E_p. Several hypotheses have been proposed to explain the decreasing trend in pan evaporation, including increasing precipitation reducing the vapor pressure deficit of the lower atmosphere, global dimming reducing shortwave radiative heating at the surface, and stilling

HESSD
11, 9435–9473, 2014

of surface winds reducing the exchange coefficient. Van Heerwaarden et al. (2010) conducted an extensive set of sensitivity tests for each of these effects on the complementary relationship using a diurnal conceptual land-boundary layer model. They concluded that "except over wet soils, the actual evapotranspiration is more sensitive to changes in soil moisture than to changes in short wave radiation so that global evaporation should have increased. Nevertheless, Wild et al. (2004) speculate that in the latter half of the 20th century, increased moisture transport from the oceans enhanced precipitation over land, but suppressed the evaporation – opposite to [their] expectations".

Figure 7 depicts the effect of an imposed 2 K warming of tropospheric column-mean temperature on E_p, E, and P. In this figure, differences between the 2 K warming configuration and the baseline are plotted against soil moisture in the baseline; also shown is the difference in soil moisture between the two prototype configurations. Across the range of baseline soil moisture conditions, the imposed warming decreases E_p (black) because q increases. While E increases under warming at low soil moisture, E decreases for soil moisture above 0.5, which corroborates the results of van Heerwaarden et al.'s (2010). In addition, precipitation (blue) increases under warming over the entire range of precipitation values (similar to Wild et al., 2004), albeit with a minimum at intermediate soil moisture values.

The opposing responses of E_p and E to warming at low soil moisture are consistent with expectations from the complementary relationship, as an increase in one corresponds to a decrease in the other. Of course, increasing the temperature increases the value of γ, which means the slope of the complementary relationship increases between the baseline and warming. On the other hand, E_wet decreases in the warming configuration, so at high soil moisture, both E_p and E decrease.

While the values of hydroclimatic variables may change substantially between the baseline and warming configurations, the Budyko curve is unchanged, as discussed in Sect. 4a. However, as Fig. 8 illustrates, points along the Budyko curve are shifted to lower aridity index values in the warming configuration compared to baseline, since

HESSD
11, 9435–9473, 2014

E_p decreases while P increases. In the energy-limited regime ($E_p/P < 1$), the ratio E/P decreases mostly because of the change in P, and since E_p also decreases, the change in E/P is smaller than E_p/P. In the water-limited regime ($E_p/P > 1$) E and E_p decrease while P increase, because of the increase in P, which directly increases the evaporative efficiency, so the percent decrease of E/P is less than that of E_p/P. Based on these results, we note the potential utility of the Budyko curve in providing qualitative or even quantitative guidance about how terrestrial hydroclimate may respond to warming.

5.2 Large-scale irrigation

Over many parts of the world, irrigation has been adopted to support agricultural production. Over India, for example, irrigation is now sufficiently extensive that large-scale alterations of hydroclimate may be occurring (Cook et al., 2010; Guimberteau et al., 2011). With respect to potential irrigation-induced changes in hydroclimate, Ozdogan et al. (2006) employed a mesoscale climate model and field data to demonstrate that large-scale irrigation in southeastern Turkey has impacted evaporation and potential evaporation in a complementary manner. They found a variety of interactions responsible for the trends, including increased atmospheric stability, decreased vapor pressure deficit, and, interestingly, a strong decrease in wind speed. Han et al. (2014) point out that while trends in E_p have often been invoked to estimate possible trends in E, how irrigation may impact E_p has typically been neglected in assessment and interpretation of E_p trends. It is thus worth briefly investigating how large-scale irrigation modulates the Budyko and complementary relationships within the framework of the prototype analyzed here. To do this, we consider the addition of an irrigation source, I, to the soil moisture balance Eq. (6), which then becomes $P + I = E + Q_{runoff}$.

To see the impact of irrigation on the prototype hydroclimate, Fig. 9 depicts E_p, E, and P as functions of soil moisture in the baseline and $I = 2\,\mathrm{mm\,day^{-1}}$ configurations. Given the direct impact of atmospheric moistening by irrigation, the transition between

HESSD
11, 9435–9473, 2014

The Budyko and complementary relationships in land–atmosphere coupling

B. R. Lintner et al.

nonprecipitating and precipitating conditions in the presence of irrigation occurs at significantly higher values of drying advection than in the non-irrigated scenario. The addition of irrigation is seen to induce a slight increase in E at a given value of soil moisture. On the other hand, since the value of drying advection is larger at a given W in the presence of irrigation, E_p itself is larger. Directly relating E_p to E indicates effectively no change in the slope of the complementary relationship, though the intercept is increased when irrigation is applied (not shown). Precipitation at a given value of W is lowered in the irrigated scenario.

As a consequence of the changes in E and P, the Budyko curve for irrigated conditions (Fig. 10, dotted line) is shifted above the baseline Budyko curve: in fact, the irrigated Budyko curve extends above 1 for aridity indices above 1 (with our prescribed irrigation flux) as water limitation is effectively alleviated. When E is replaced by $E^* = E - I$, the resulting Budyko-like curve (stars) drops below the baseline.

Of course, we should point out that by imposing irrigation in the prototype at fixed tropospheric temperature, we are neglecting a potentially important cooling of the lowermost atmosphere, not to mention that our prototype does not account for changes in convective initiation or triggering that may occur, e.g., through increased low-level stability. Thus, the irrigation impacts described here merely reflect the direct effect of added moisture to the atmosphere. Moreover, we do not take into account vegetation control on E since we only represent soil moisture limitation on evapotranspiration through a bucket model.

6 Summary and conclusions

In this study, we use an idealized prototype incorporating the key physics of large-scale land–atmosphere coupling to derive analytic expressions for the well-known Budyko and complementary relationships. Our approach differs from previous analytic approaches in that precipitation and moisture convergence are treated implicitly rather than applied as an external forcing. The analytic solutions permit straightforward

HESSD
11, 9435–9473, 2014

diagnosis of the sensitivity of the Budyko and complementary relationships to atmospheric and land surface parameters. In particular, the slope of the complementary relationship is shown to be mostly dependent on the temperature with important implications for the continental hydrologic cycle with a warming climate. One consequence of this dependence is that the complementary relationship may be expected to become more asymmetric with warming, as higher values of the slope imply a larger change in potential evaporation for a given change in evapotranspiration. On the other hand the Budyko curve is very stable to many parameterization of the model parameters or global temperature. It is thus expected that the Budyko curve should remain relatively stable under a warming climate. Other causes of anthropogenic changes such as large-scale irrigation are however shown to strongly impact the Budyko curve with little impact on the complementary relationship.

Acknowledgements. This work was supported by National Science Foundation (NSF) grant AGS-1035968 and New Jersey Agricultural Experiment Station Hatch grant NJ07102.

References

Allen, M. R. and Ingram, W. J.: Constraints on future changes in climate and the hydrologic cycle, Nature, 419, 224–232, doi:10.1038/nature01092, 2002.

Betts, A. K.: Coupling of water vapor convergence, clouds, precipitation, and land-surface processes, J. Geophys. Res.-Atmos., 112, D10108, doi:10.1029/2006JD008191, 2007.

Betts, A. K., Desjardins, R., Worth, D., Wang, S., and Li, J.: Coupling of winter climate transitions to snow and clouds over the Prairies, J. Geophys. Res.-Atmos., 119, 1118–1139, doi:10.1002/2013JD021168, 2014.

Betts, A. K. and Viterbo, P.: Land-surface, boundary layer, and cloud-field coupling over the southwestern Amazon in ERA-40, J. Geophys. Res.-Atmos., 110, 1–15, doi:10.1029/2004JD005702, 2005.

Betts, A. K., Ball, J., Beljaars, A., Miller, M. J., and Viterbo, P.: The land surface–atmosphere interaction: a review based on observational and global modeling perspectives, J. Geophys. Res.-Atmos., 101, 7209–7225, 1996.

HESSD
11, 9435–9473, 2014
The Budyko and complementary relationships in land–atmosphere coupling
B. R. Lintner et al.

Title Page
Abstract | Introduction
Conclusions | References
Tables | Figures
◂| |▸
◂ ▸
Back | Close
Full Screen / Esc
Printer-friendly Version
Interactive Discussion

Betts, A. K., Ball, J. H., Bosilovich, M., Viterbo, P., and Zhang, Y.: Intercomparison of water and energy budgets for five Mississippi subbasins between ECMWF reanalysis (ERA-40) and NASA Data Assimilation Office GCM for 1990, J. Geophys. Res.-Atmos., 108, 8618, doi:10.1029/2002JD003127, 2003.

Bosman, H. H.: The influence of installation practices on evaporation from Symon's tank and American Class A-pan evaporimeters, Agr. Forest Meteorol., 41, 307–323, 1987.

Bouchet, R.: Evapotranspiration reelle et potentielle, signification climatique, IAHS Publ., 62, 134–142, 1963.

Brutsaert, W. and Parlange, M. B.: Hydrologic cycle explains the evaporation paradox, Nature, 396, 29–30, 1998.

Brutsaert, W. and Stricker, H.: An advection-aridity approach to estimate actual regional evapotranspiration, Water Resour. Res., 15, 443–450, 1979.

Budyko, M. I.: The heat and water balance of the Earth's surface, the general theory of physical geography and the problem of the transformation of nature, Sov. Geogr., 2, 3–12, doi:10.1080/00385417.1961.10770737, 1961.

Budyko, M. I.: Climate and Life, Academic Press, Orlando, FL, 508 pp., 1974.

Cook, B. I., Puma, M. J., and Krakauer, N. Y.: Irrigation induced surface cooling in the context of modern and increased greenhouse gas forcing, Clim. Dynam., 37, 1587–1600, doi:10.1007/s00382-010-0932-x, 2010.

Crago, R. and Crowley, R.: Complementary relationships for near-instantaneous evaporation, J. Hydrol., 300, 199–211, doi:10.1016/j.jhydrol.2004.06.002, 2005.

Dirmeyer, P. A., Cash, B. A., Kinter III, J. L., Stan, C., Jung, T., Marx, L., Towers, P., Wedi, N., Adams, J. M., Altshuler, E. L., Huang, B., Jin, E. K., and Manganello, J.: Evidence for enhanced land–atmosphere feedback in a warming climate, J. Hydrometeorol., 13, 981–995, doi:10.1175/JHM-D-11-0104.1, 2012.

Dirmeyer, P. A., Wang, Z., Mbuh, M. J., and Norton, H. E.: Intensified land surface control on boundary layer growth in a changing climate, Geophys. Res. Lett., 41, W04403, doi:10.1002/2013GL058826, 2014.

Donohue, R. J., Roderick, M. L., and McVicar, T. R.: On the importance of including vegetation dynamics in Budyko's hydrological model, Hydrol. Earth Syst. Sci., 11, 983–995, doi:10.5194/hess-11-983-2007, 2007.

Eagleson, P.: Climate, soil, and vegetation, 2. The distribution of annual precipitation derived from observed storm sequences, Water Resour Res., 14, 713–721, 1978a.

Eagleson, P.: Climate, soil, and vegetation, 6. Dynamics of the annual water balance, Water Resour. Res., 14, 749–764, 1978b.
Eagleson, P.: Climate, soil, and vegetation, 1. Introduction to water balance dynamics, Water Resour. Res., 14, 705–712, 1978c.
Fu, B. P.: On the calculation of the evaporation from land surface, Sci. Atmos. Sin, 5, 23–31, 1981.
Gentine, P., Entekhabi, D. D., and Polcher, J.: The diurnal behavior of evaporative fraction in the soil-vegetation-atmospheric boundary layer continuum, J. Hydrometeorol., 12, 1530–1546, doi:10.1175/2011JHM1261.1, 2011.
Gentine, P., D'Odorico, P., Lintner, B. R., Sivandran, G., and Salvucci, G.: Interdependence of climate, soil, and vegetation as constrained by the Budyko curve, Geophys. Res. Lett., 39, L19404, doi:10.1029/2012GL053492, 2012.
Gerrits, A. M. J., Savenije, H. H. G., Veling, E. J. M., and Pfister, L.: Analytical derivation of the Budyko curve based on rainfall characteristics and a simple evaporation model, Water Resour. Res., 45, W04403, doi:10.1029/2008WR007308, 2009.
Granger, R. J.: A complementary relationship approach for evaporation from nonsaturated surfaces, J. Hydrol., 111, 31–38, 1989.
Guimberteau, M., Laval, K., Perrier, A., and Polcher, J.: Global effect of irrigation and its impact on the onset of the Indian summer monsoon, Clim. Dynam., 39, 1329–1348, doi:10.1007/s00382-011-1252-5, 2011.
Han, S., Tang, Q., Xu, D., and Wang, S.: Irrigation-induced changes in potential evaporation: more attention is needed, Hydrol. Process., 28, 2717–2720, doi:10.1002/hyp.10108, 2014.
Harman, C. J., Troch, P. A., and Sivapalan, M.: Functional model of water balance variability at the catchment scale: 2. Elasticity of fast and slow runoff components to precipitation change in the continental United States, Water Resour. Res., 47, W02523, doi:10.1029/2010WR009656, 2011.
Held, I. M. and Soden, B. J.: Robust response of the hydrological cycle to global warming, J. Climate, 19, 5686–5699, 2006.
Hobbins, M. T., Ramirez, J. A., Brown, T. C., and Claessens, L. H. J. M.: The complementary relationship in estimation of regional evapotranspiration: the complementary relationship area evapotranspiration and advection-aridity models, Water Resour. Res., 37, 1367–1387, 2001.

Hobbins, M. T., Ramirez, J. A., and Brown, T. C.: Trends in pan evaporation and actual evapotranspiration across the conterminous US: paradoxical or complementary?, Geophys. Res. Lett., 31, L13503, doi:10.1029/2004GL019846, 2004.
Istanbulluoglu, E., Wang, T., Wright, O. M., and Lenters, J. D.: Interpretation of hydrologic trends from a water balance perspective: the role of groundwater storage in the Budyko hypothesis, Water Resour. Res., 48, W00H16, doi:10.1029/2010WR010100, 2012.
Kahler, D. M. and Brutsaert, W.: Complementary relationship between daily evaporation in the environment and pan evaporation, Water Resour. Res., 42, W05413, doi:10.1029/2005WR004541, 2006.
Kleidon, A. and Heimann, M.: A method of determining rooting depth from a terrestrial biosphere model and its impacts on the global water and carbon cycle, Global Change Biol., 4, 275–286, 1998.
Koster, R. and Suarez, M.: A simple framework for examining the interannual variability of land surface moisture fluxes, J. Climate, 12, 1911–1917, 1999.
Koster, R. D., Dirmeyer, P. A., Guo, Z., Bonan, G., Chan, E., Cox, P., Davies, H., Gordon, T., Kanae, S., Kowalczyk, E., Lawrence, D., Liu, P., Lu, S., Malyshev, S., McAvaney, B., Mitchell, K., Oki, T., Oleson, K., Pitman, A., Sud, Y., Taylor, C., Verseghy, D., Vasic, R., Xue, Y., and Yamada, T.: Regions of strong coupling between soil moisture and precipitation, Science, 305, 1138–1140, 2004.
Koster, R. D., Guo, Z., Dirmeyer, P. A., Bonan, G., Chan, E., Cox, P., Davies, H., Gordon, T., Kanae, S., Kowalczyk, E., Lawrence, D., Liu, P., Lu, S. Malyshev, S., McAvaney, B., Mitchell, K., Oki, T., Oleson, K., Pitman, A., Sud, Y., Taylor, C., Verseghy, D., Vasic, R., Xue, Y., and Yamada, T.: GLACE: the Global Land–Atmosphere Coupling Experiment, Part I: Overview, J. Hydrometeorol., 7, 590–610, 2006.
Kirchner, J. W.: Catchments as simple dynamical systems: catchment characterization, rainfall–runoff modeling, and doing hydrology backward, Water Resour. Res., 45, W02429, doi:10.1029/2008WR006912, 2009.
Lawrimore, J. and Peterson, T.: Pan evaporation trends in dry and humid regions of the United States, J. Hydrometeorol., 1, 543–546, 2000.
Lee, J.-E., Lintner, B. R., Boyce, C. K., and Lawrence, P. J.: Land use change exacerbates tropical South American drought by sea surface temperature variability, Geophys. Res. Lett., 38, L19706, doi:10.1029/2011GL049066, 2011.

HESSD
11, 9435–9473, 2014

The Budyko and complementary relationships in land–atmosphere coupling

B. R. Lintner et al.

Lettau, H.: Evapotranspiration climatonomy, I. A new approach to numerical prediction of monthly evapotranspiration, runoff, and soil moisture storage, Mon. Weather Rev., 97, 691–699, 1969.
L'homme, J. and Guilioni, L.: Comments on some articles about the complementary relationship, J. Hydrol., 323, 1–3, doi:10.1016/j.jhydrol.2005.08.014, 2006.
Lintner, B. R., Gentine, P., Findell, K. L., D'Andrea, F., Sobel, A. H., and Salvucci, G. D.: An idealized prototype for large-scale land–atmosphere coupling, J. Climate, 26, 2379–2389, doi:10.1175/JCLI-D-11-00561.1, 2013.
Manzoni, S., Vico, G., Katul, G., Fay, P. A., Polley, W., Palmroth, S., and Porporato, A.: Optimizing stomatal conductance for maximum carbon gain under water stress: a meta-analysis across plant functional types and climates, Funct. Ecol., 25, 456–467, doi:10.1111/j.1365-2435.2010.01822.x, 2011.
Milly, P. C. D.: Climate, soil water storage, and the average annual water balance, Water Resour. Res., 30, 2143–2156, 1994.
Milly, P. C. D. and Dunne, K.: Macroscale water fluxes – 2. Water and energy supply control of their interannual variability, Water Resour. Res., 38, 1206, doi:10.1029/2001WR000760, 2002.
Milly, P. C. D., Dunne, K., and Vecchia, A. V.: Global pattern of trends in streamflow and water availability in a changing climate, Nature, 438, 347–350, doi:10.1038/nature04312, 2005.
Morton, F. I.: Operational estimates of areal evapotranspiration and their significance to the science and practice of hydrology, J. Hydrol., 66, 1–76, 1983.
Neelin, J. D. and Zeng, N.: A quasi-equilibrium tropical circulation model – formulation, J. Atmos. Sci., 57, 1741–1766, 2000.
Neelin, J. D., Munnich, M., Su, H., Meyerson, J., and Holloway, C.: Tropical drying trends in global warming models and observations, P. Natl. Acad. Sci. USA, 103, 6110–6115, 2006.
Ozdogan, M., Salvucci, G., and Anderson, B.: Examination of the Bouchet-Morton complementary relationship using a mesoscale climate model and observations under a progressive irrigation scenario, J. Hydrometeorol., 7, 235–251, 2006.
Pettijohn, J. C. and Salvucci, G. D.: A new two-dimensional physical basis for the complementary relation between terrestrial and pan evaporation, J. Hydrometeorol., 10, 565–574, doi:10.1175/2008JHM1026.1, 2009.

Porporato, A., Laio, F., Ridolfi, L., and Rodrìguez-Iturbe, I.: Plants in water-controlled ecosystems: active role in hydrologic processes and response to water stress – III. Vegetation water stress, Adv. Water Resour., 24, 725–744, 2001.

Porporato, A., Daly, E., and Rodr ìguez-Iturbe, I.: Soil water balance and ecosystem response to climate change, Am. Nat., 164, 625–632, 2004.

Potter, N., Zhang, L., Milly, P., McMahon, T., and Jakeman, A.: Effects of rainfall seasonality and soil moisture capacity on mean annual water balance for Australian catchments, Water Resour. Res., 41, W06007, doi:10.1029/2004WR003697, 2005.

Priestley, C. H. B. and Taylor, R. J.: On the assessment of surface heat flux and evaporation using large-scale parameters, Mon. Weather Rev., 100, 81–88, 1972.

Ramirez, J. A., Hobbins, M. T., and Brown, T. C.: Observational evidence of the complementary relationship in regional evaporation lends strong support for Bouchet's hypothesis, Geophys. Res. Lett., 32, L15401, doi:10.1029/2005GL023549, 2005.

Roderick, M. L. and Farquhar, G. D.: Changes in Australian pan evaporation from 1970 to 2002, Int. J. Climatol., 24, 1077–1090, doi:10.1002/joc.1061, 2004.

Roderick, M. L. and Farquhar, G. D.: A simple framework for relating variations in runoff to variations in climatic conditions and catchment properties, Water Resour. Res., 47, W00G07, doi:10.1029/2010WR009826, 2011.

Seneviratne, S. I., Koster, R. D., Guo, Z., Dirmeyer, P. A., Kowalczyk, E., Lawrence, D., Liu, P., Lu, C.-H., Mocko, D., Oleson, K. W., and Verseghy, D.: Soil moisture memory in AGCM simulations: analysis of Global Land–Atmosphere Coupling Experiment (GLACE) data, J. Hydrometeorol., 7, 1090–1112, 2006.

Shen, Y., Liu, C., Liu, M., Zeng, Y., and Tian, C.: Change in pan evaporation over the past 50 years in the arid region of China, Hydrol. Process., 24, 225–231, doi:10.1002/hyp.7435, 2009.

Sherwood, S. and Fu, Q.: A drier future?, Science, 343, 737–739, doi:10.1126/science.1247620, 2014.

Sivapalan, M., Yaeger, M. A., Harman, C. J., Xu, X., and Troch, P. A.: Functional model of water balance variability at the catchment scale: 1. Evidence of hydrologic similarity and space–time symmetry, Water Resour. Res., 47, W02522, doi:10.1029/2010WR009568, 2011.

Sobel, A. H. and Bretherton, C. S.: Modeling tropical precipitation in a single column, J. Climate, 13, 4378–4392, 2000.

Sobel, A. H., Nilsson, J., and Polvani, L.: The weak temperature gradient approximation and balanced tropical moisture waves, J. Atmos. Sci., 58, 3650–3665, 2001.
Szilagyi, J.: On Bouchet's complementary hypothesis, J. Hydrol., 246, 155–158, 2001.
Szilagyi, J.: On the inherent asymmetric nature of the complementary relationship of evaporation, Geophys. Res. Lett., 34, L02405, doi:10.1029/2006GL028708, 2007.
Szilagyi, J. and Jozsa, J.: Complementary relationship of evaporation and the mean annual water-energy balance, Water Resour. Res., 45, W09201, doi:10.1029/2009WR008129, 2009.
Troch, P. A., Martinez, G. F., Pauwels, V. R. N., Durcik, M., Sivapalan, M., Harman, C., Brooks, P. D., Gupta, H., and Huxman, T.: Climate and vegetation water use efficiency at catchment scales, Hydrol. Process., 23, 2409–2414, doi:10.1002/hyp.7358, 2009.
Tuttle, S. E. and Salvucci, G. D.: A new method for calibrating a simple, watershed-scale model of evapotranspiration: maximizing the correlation between observed streamflow and model-inferred storage, Water Resour. Res., 48, W05556, doi:10.1029/2011WR011189, 2012.
van Heerwaarden, C. C., Vilà-Guerau de Arellano, J., and Teuling, A. J.: Land–atmosphere coupling explains the link between pan evaporation and actual evapotranspiration trends in a changing climate, Geophys. Res. Lett., 37, L21401, doi:10.1029/2010GL045374, 2010.
Wild, M., Ohmura, A., Gilgen, H., and Rosenfeld, D.: On the consistency of trends in radiation and temperature records and implications for the global hydrological cycle, Geophys. Res. Lett., 31, L11201, doi:10.1029/2003GL019188, 2004.
Williams, C. A., Reichstein, M., Buchmann, N., Baldocchi, D., Beer, C., Schwalm, C., Wohlfahrt, G., Hasler, N., Bernhofer, C., Foken, T., Papale, D., Schymanski, S., and Schaefer, K.: Climate and vegetation controls on the surface water balance: synthesis of evapotranspiration measured across a global network of flux towers, Water Resour. Res., 48, W06523, doi:10.1029/2011WR011586, 2012.
Yang, D., Sun, F., Liu, Z., Cong, Z., Ni, G., and Lei, Z.: Analyzing spatial and temporal variability of annual water-energy balance in nonhumid regions of China using the Budyko hypothesis, Water Resour. Res., 43, W04426, doi:10.1029/2006WR005224, 2007.
Yang, D., Shao, W., Yeh, P. J.-F., Yang, H., Kanae, S., and Oki, T.: Impact of vegetation coverage on regional water balance in the nonhumid regions of China, Water Resour. Res., 45, W00A14, doi:10.1029/2008WR006948, 2009.

HESSD
11, 9435–9473, 2014

Yang, H., Yang, D., Lei, Z., and Sun, F.: New analytical derivation of the mean annual water-energy balance equation, Water Resour. Res., 44, W03410, doi:10.1029/2007WR006135, 2008.

Zanardo, S., Harman, C. J., Troch, P. A., Rao, P. S. C., and Sivapalan, M.: Intra-annual rainfall variability control on interannual variability of catchment water balance: a stochastic analysis, Water Resour. Res., 48, W00J16, doi:10.1029/2010WR009869, 2012.

Zeng, N., Neelin, J. D., and Chou, C.: A quasi-equilibrium tropical circulation model – implementation and simulation, J. Atmos. Sci., 57, 1767–1796, 2000.

Zhang, L., Hickel, K., Dawes, W., Chiew, F., Western, A., and Briggs, P.: A rational function approach for estimating mean annual evapotranspiration, Water Resour. Res., 40, W02502, doi:10.1029/2003WR002710, 2004.

Table 1. Parameter definitions and values in the baseline land–atmosphere coupling prototype.

Parameter	Definition	Value
a_{1s}	Weighting factor for surface temperature	0.30
α	Priestly–Taylor coefficient	1.26
b_{1s}	Weighting factor for surface moisture	1.15
b	Complementary relationship scale factor	–
c_{surf}	Surface cloud longwave forcing coefficient	0.18
γ	Dimensionless slope of Clausius–Clapeyron relationship	3.5
ε_H	Linearized surface turbulent flux scaling coefficient	42 mm day^{-1} K^{-1}
η	Runoff power law scaling exponent	4
τ_c	Convective adjustment timescale	2 h

HESSD
11, 9435–9473, 2014

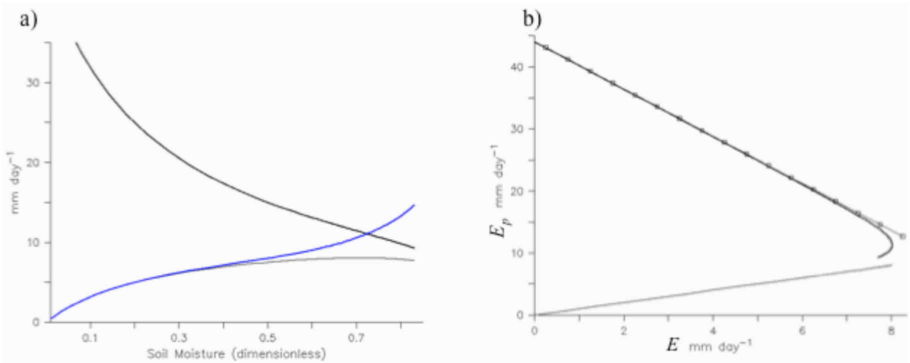

Figure 1. Complementary relationship in the baseline configuration. **(a)** Potential evapotranspiration (E_p; black), evapotranspiration (E; gray), and precipitation (P; blue) as functions of soil moisture (W). **(b)** E_p vs. E (black) and the 1 : 1 line (gray). Also shown is the best fit linear regression of the E_p to E relationship (squares).

HESSD

11, 9435–9473, 2014

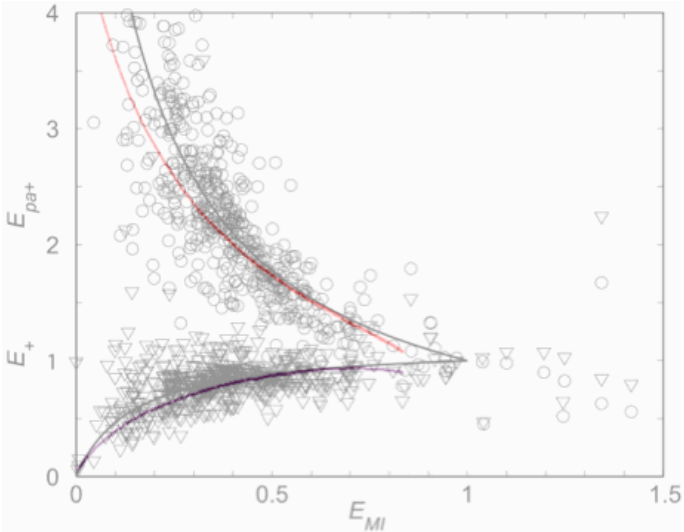

Figure 2. Baseline complementary relationship compared to Kahler and Brutsaert's observational data from the Little Washita River basin in Oklahoma, USA (c.f., Fig. 5 in Kahler and Brutsaert, 2006). Symbols shown correspond to two different normalizations of the observations and gray lines to best fits through these points. Prototype E_p and E (red and purple curves, respective) have been normalized with respect to the value of E_{wet} corresponding to the maximum value of E along the transect.

HESSD
11, 9435–9473, 2014

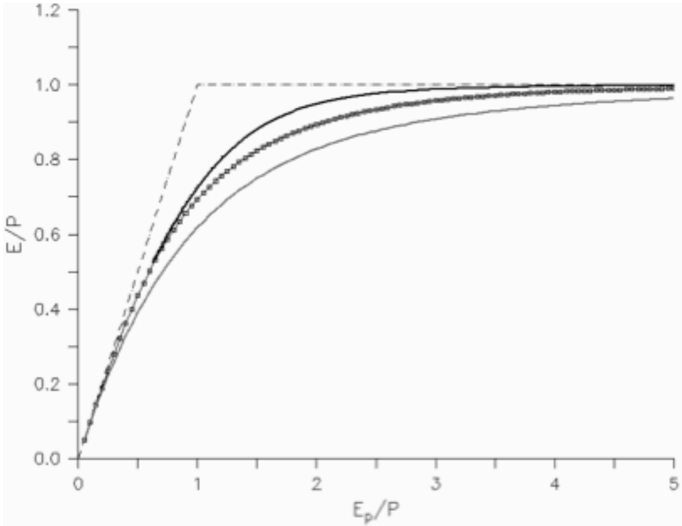

Figure 3. Prototype Budyko curves for the baseline prototype, i.e., $\eta = 4$ in the formulation of runoff (thick black), for Eq. (8) for $\eta = 2$ (gray), and Budyko's empirical formulation (squares). The dashed lines are the energy- and water-limited asymptotes.

HESSD
11, 9435–9473, 2014

Title Page
Abstract | Introduction
Conclusions | References
Tables | Figures
Back | Close
Full Screen / Esc
Printer-friendly Version
Interactive Discussion

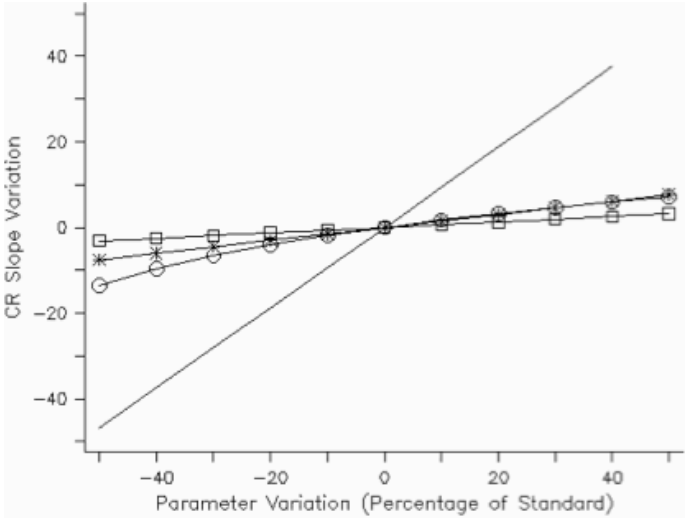

Figure 4. Parameter sensitivity of the complementary relationship slope. Results shown are for varying: the slope of the saturation specific humidity with respect to temperature (no symbols), surface drag coefficient (circles), surface cloud radiative forcing (stars), and convective adjustment timescale (squares).

HESSD
11, 9435–9473, 2014

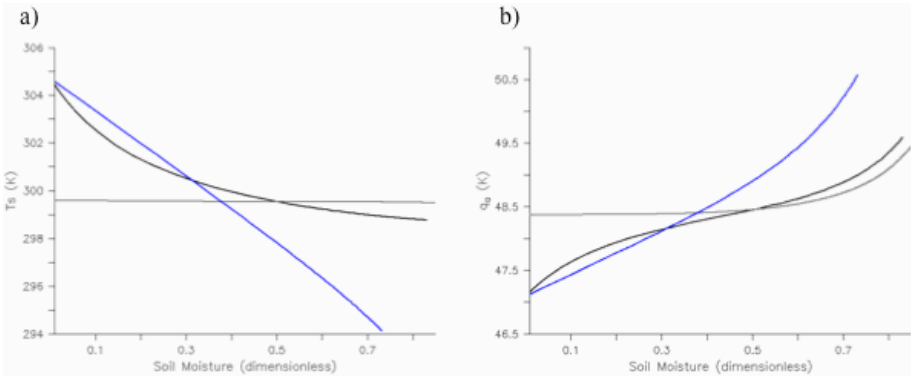

Figure 5. Comparison of prototype **(a)** surface temperature T_s and **(b)** surface air humidity q_a for the baseline (black), fixed β (gray), and fixed E_p (blue) configurations of the prototype. Note that q_a is converted to temperature units of K.

HESSD
11, 9435–9473, 2014

The Budyko and complementary relationships in land–atmosphere coupling

B. R. Lintner et al.

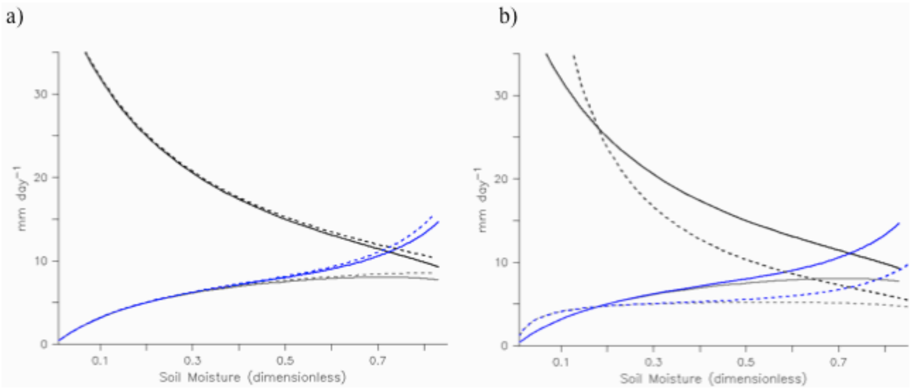

Figure 6. Impact on the complentary relationship from prescribing either **(a)** net surface radiative heating or **(b)** sensible heat flux. The curves depicted correspond to E_p (black), E (gray), and P (blue) for the baseline configuration (solid) and prescribed radiative or sensible heat fluxes (dashed).

HESSD
11, 9435–9473, 2014

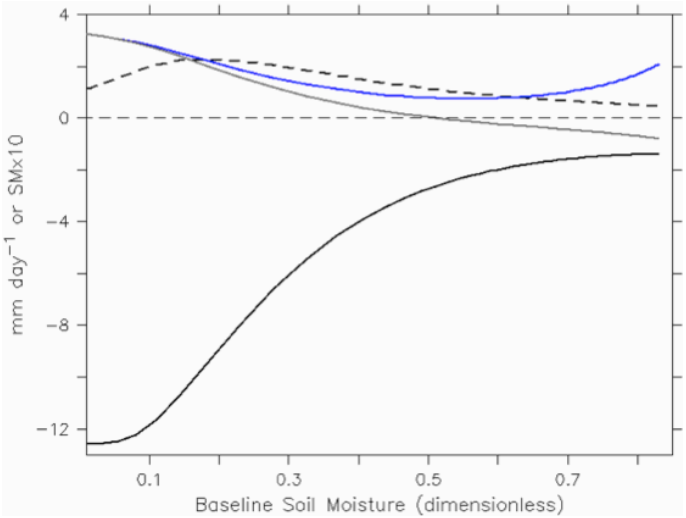

Figure 7. Differences in E_p (black), E (gray), and P (blue) for a +2 K warming relative to the baseline configuration as functions of soil moisture in the baseline configuration. Also shown is the difference in soil moisture (dashed black), which has been rescaled by a factor of 10.

HESSD
11, 9435–9473, 2014

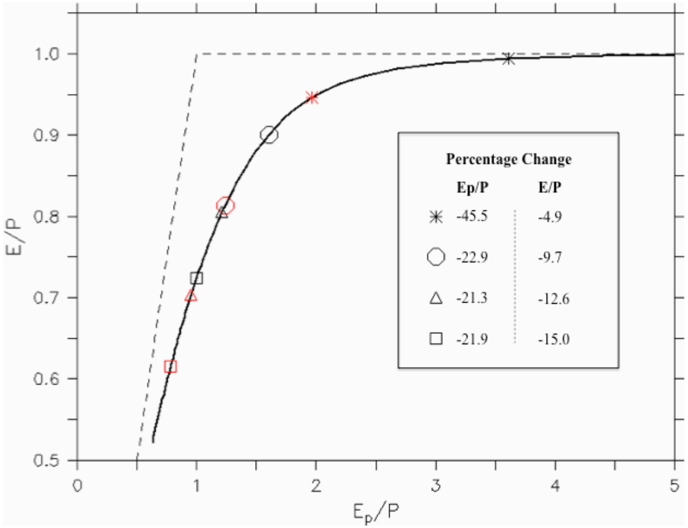

Figure 8. Shift in selected points along the Budyko curve for the baseline (black symbols) and +2 K warming (red) configuration. Pairs of like shaped symbols correspond to the same level of imposed drying advection forcing. The values shown in the inset are the percentage changes for each of the baseline and +2 K warming pairs.

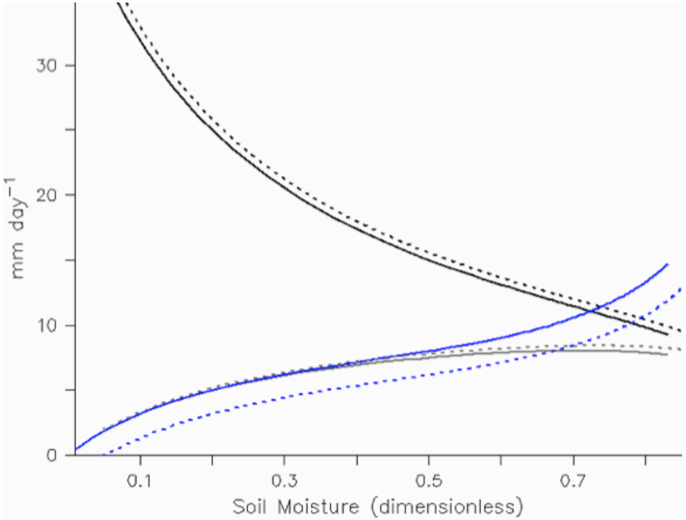

Figure 9. Comparison of E_p (black), E (gray), and P (blue) as functions of W for the baseline (solid curves) and $I = 2\,\mathrm{mm\,day^{-1}}$ (dotted curves) configurations.

HESSD
11, 9435–9473, 2014

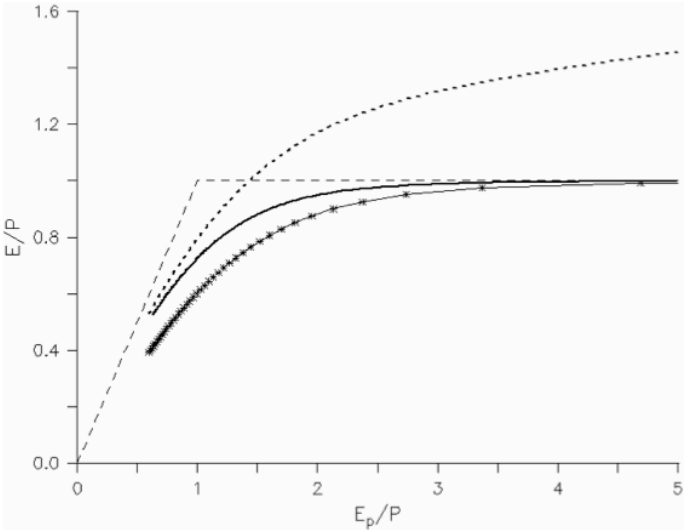

Figure 10. Comparison of Budyko curves for the baseline (solid) and $I = 2\,\mathrm{mm\,day^{-1}}$ (dotted) configurations. Also shown is a Budyko-like curve in which E is replaced by $E^* = E - I$ (stars).

HESSD
11, 9435–9473, 2014

The Budyko and complementary relationships in land–atmosphere coupling

B. R. Lintner et al.